Langmuir

Article

Preparation of Well-Defined Core#Shell Particles by Cu-Mediated Graft Copolymerization of Methyl Methacrylate from Bovine Serum Albumin

Chuanxin He, Jianhong Liu, Xiaodong Ye, Laiyong Xie, Qianling Zhang, Xiangzhong Ren, Guangzhao Zhang, and Chi Wu

Langmuir, **2008**, 24 (19), 10717-10722 • DOI: 10.1021/la801132r • Publication Date (Web): 13 September 2008

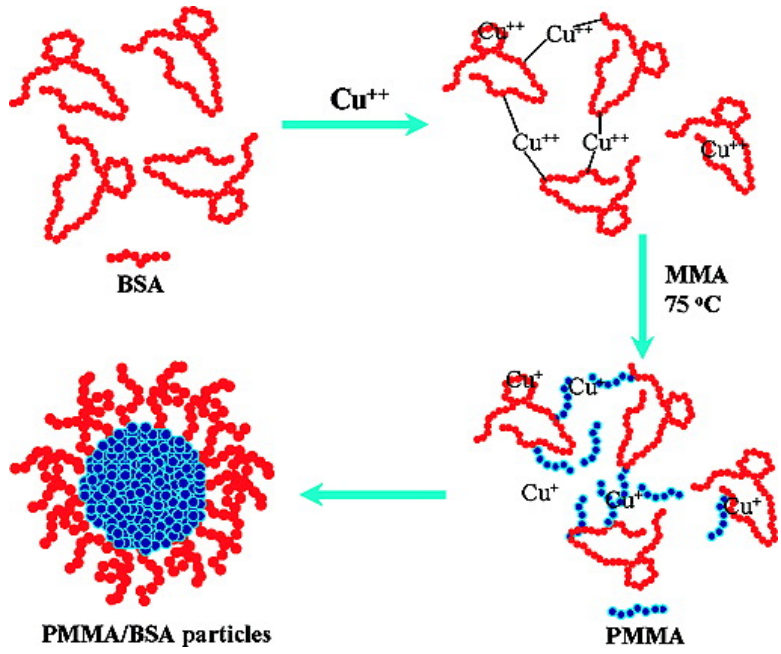

More About This Article

Additional resources and features associated with this article are available within the HTML version:

- Supporting Information
- Access to high resolution figures
- Links to articles and content related to this article
- Copyright permission to reproduce figures and/or text from this article

View the Full Text HTML

Langmuir is published by the American Chemical Society. 1155 Sixteenth Street N.W., Washington, DC 20036

Preparation of Well-Defined Core−Shell Particles by Cu^{2+}-Mediated Graft Copolymerization of Methyl Methacrylate from Bovine Serum Albumin

Chuanxin He,[†,‡] Jianhong Liu,*[,‡] Xiaodong Ye,[†] Laiyong Xie,[†] Qianling Zhang,[‡] Xiangzhong Ren,[‡] Guangzhao Zhang,[†] and Chi Wu[†,§]

The Hefei National Laboratory for Physical Sciences at Microscale and Department of Chemical Physics, University of Science and Technology of China, Hefei, Anhui 230026, China, School of Chemistry and Chemical Engineering, Shenzhen University, Shenzhen, Guangdong 518060, China, and Department of Chemistry, The Chinese University of Hong Kong, Shatin, N.T., Hong Kong

Received April 10, 2008. Revised Manuscript Received July 7, 2008

Small well-defined core−shell poly(methyl methacrylate)−bovine serum albumin (PMMA-BSA) particles have been prepared in a direct one-step graft copolymerization of MMA from BSA at 75 °C in water with a trace amount of Cu^{2+} (5 μM). Initially, BSA generates free radicals and acts as a multifunctional macroinitiator, which leads to the formation of an amphiphilic PMMA-BSA grafting copolymer. Such formed copolymer chains act as a polymeric stabilizer to promote further emulsion polymerization of MMA inside, resulting in surfactant-free stable core−shell particles, confirmed by a transmission electron microscopic (TEM) analysis. The PMMA-BSA copolymers as well as PMMA homopolymer inside the particles were isolated by Soxhlet extraction and characterized by Fourier transform infrared spectroscopy (FT-IR) and thermogravimetry (TG). The highest grafting efficiency was ∼80%. Effects of the reaction temperature, the MMA/BSA ratio, and the concentrations of Cu^{2+} and BSA on such core−shell particle formation have been systematically studied. Due to their inert PMMA core and biocompatible BSA shell, these small polymer particles are potentially useful in biomedical applications.

Introduction

Bovine serum albumin (BSA) is the most abundant globular protein in plasma. It consists of 583 amino acids in a single polypeptide chain.[1] X-ray scattering and laser light scattering (LLS) experiments reveal that BSA is an oblate ellipsoid with dimensions of (14 nm × 4 nm).[2,3] ^{1}H NMR and X-ray crystallography further confirm its heart-shaped structure.[4,5] As a biodegradable and biocompatible macromolecule, BSA is relatively nontoxic and nonimmunogenic.[6,7] Its suitability in biomedical applications has been extensively studied.[8−11] Seliktar et al.[12] reported some PEG−albumin conjugates for the formation of photopolymerizable biomimetic hydrogels for tissue engineering. Chehimi et al.[13−15] prepared some core−shell particles with an active ester-functionalized polypyrrole shell. It has been shown that these particles were effective for the covalent immobilization of human serum albumin (HSA) and the recognition of anti-HSA by HSA-decorated particles. Latexes obtained in this way were suitable for visual diagnostic assays.

The graft copolymerization of various monomers onto biopolymers has been investigated and reported with different initiation methods. Most of them have dealt with the synthesis of water-soluble copolymers; only a few past studies have been focused on the one-step formation of stable core−shell particles and their applications.[16−18] Previous initiation methods led to lots of homopolymer chains, and the grafting efficiency is less than 50%. On the other hand, BSA can be cross-linked by glutaraldehyde or formaldehyde via its functional (carboxyl and amino) groups.[19−21] Iemma et al.[22,23] showed a chemical modification of BSA by introducing unsaturated groups and then used it as a macromonomer to prepare spherical microparticles by radical copolymerization. Recently, several groups reported

* To whom correspondence should be addressed.
† University of Science and Technology of China.
‡ Shenzhen University.
§ The Chinese University of Hong Kong.

(1) Valstar, A.; Vasilescu, M.; Vigouroux, C.; Stilbs, P.; Almgren, M. *Langumir* **2001**, *17*, 3208–3215.
(2) Bloomfield, V. *Biochemistry* **1966**, *5*, 684–689.
(3) Squire, P. G.; Moser, P.; O'Konski, C. T. *Biochemistry* **1968**, *7*, 4261–4272.
(4) Bos, O. J. M.; Labro, J. F. A.; Fischer, M. J. E.; Wilting, J.; Janssen, L. H. M. *J. Biol. Chem.* **1989**, *264*, 953–959.
(5) Carter, D. C.; He, X. M.; Munson, S. H.; Twigg, P. D.; Gernert, K. M.; Broom, M. B.; Miller, T. Y. *Science* **1989**, *244*, 1195–1198.
(6) Langer, K.; Balthasar, S.; Vogel, V.; Dinauer, N.; von Briesen, H.; Schubert, D. *Int. J. Pharm.* **2003**, *257*, 169–180.
(7) Arnedo, A.; Espuelas, S.; Irache, J. M. *Int. J. Pharm.* **2002**, *244*, 59–72.
(8) Norde, W.; Gage, D. *Langmuir* **2004**, *20*, 4162–4167.
(9) Shcharbin, D.; Pedziwiatr, E.; Chonco, L.; Bermejo-Martin, J. F.; Ortega, P.; de la Mata, F. J.; Eritja, R.; Gomez, R.; Klajnert, B.; Bryszewska, M.; Munoz-Fernandez, M. A. *Biomacromolecules* **2007**, *8*, 2059–2062.
(10) Melillo, M.; Gun'ko, V. M.; Tennison, S. R.; Mikhalovska, L. I.; Phillips, J. G.; Davies, G. J.; Lloyd, A. W.; Kozynchenko, O. P.; Malik, D. J.; Streat, M.; Mikhalovsky, S. V. *Langmuir* **2004**, *20*, 2837–2851.
(11) Wittemann, A.; Azzam, T.; Eisenberg, A. *Langmuir* **2007**, *23*, 2224–2230.
(12) Gonen-Wadmany, M.; Oss-Ronen, L.; Seliktar, D. *Biomaterials* **2007**, *28*, 3876–3886.
(13) Azioune, A.; Ben Slimane, A.; Ait Hamou, L.; Pleuvy, A.; Chehimi, M. M.; Perruchot, C.; Armes, S. P. *Langmuir* **2004**, *20*, 3350–3356.
(14) Benabderrahmane, S.; Bousalem, S.; Mangeney, C.; Azioune, A.; Vaulay, M.-J.; Chehimi, M. M. *Polymer* **2005**, *46*, 1339–1346.
(15) Bousalem, S.; Benabderrahmane, S.; Cheung Sang, Y. Y.; Mangeney, C.; Chehimi, M. M. *J. Mater. Chem.* **2005**, *15*, 3109–3116.
(16) Li, P.; Liu, J. H.; Wang, Q.; Wu, C. *Macromol. Symp.* **2000**, *151*, 605–610.
(17) Li, P.; Zhu, J.; Sunintaboon, P.; Harris, F. W. *Langmuir* **2002**, *18*, 8641–8646.
(18) Zhu, J.; Li, P. *J. Polym. Sci., Part A: Polym. Chem.* **2003**, *41*, 3346–3353.
(19) Merodio, M.; Arnedo, A.; Renedo, M. J.; Irache, J. M. *Eur. J. Pharm. Sci.* **2001**, *12*, 251–259.
(20) Lei, C.; Deng, J. *Anal. Chem.* **1996**, *68*, 3344–3349.
(21) Tome, D.; Kozlowski, A.; Mabon, F. *J. Agric. Food Chem.* **1985**, *33*, 449–455.
(22) Iemma, F.; Spizzirri, U. G.; Muzzalupo, R.; Puoci, F.; Trombino, S.; Picci, N. *Colloid Polym. Sci.* **2004**, *283*, 250–256.
(23) Iemma, F.; Spizzirri, U. G.; Francesco, P.; Muzzalupo, R.; Trombino, S.; Cassano, R.; Leta, S.; Picci, N. *Int. J. Pharm.* **2006**, *312*, 151–157.

10.1021/la801132r CCC: $40.75
Published on Web 09/13/2008

that BSA can conjugate with polymers by living free-radical polymerization. For example, Maynard et al.[24,25] first made BSA as an atom transfer radical polymerization (ATRP) macroinitiator and then use it to prepare BSA−polymer conjugates. Further, Bulmus et al.[26] and Davis et al.[27] use the reversible addition−fragmentation chain transfer polymerization (RAFT), starting with the preparation of a BSA-macroRAFT agent, to synthesize a water-soluble copolymer at room temperature. These previous studies involve multiple steps, including synthesis, chemical modification, purification, and conjugation. To our knowledge, the preparation of stable BSA/PMMA core−shell particles by the copper-mediated graft copolymerization has not yet been reported. Most importantly, the preparation of polymer−BSA particles has not been systematically studied. Note that small stable particles with a BSA shell could be used to immobilize other biomacromolecules, such as antibody, enzyme, and DNA. This study is mainly designed to find some optimal reaction conditions for the one-step preparation of small well-defined amphiphilic core−shell PMMA−BSA spheres via the graft copolymerization of methyl methacrylate from BSA without any surfactant. The current study has laid the groundwork for our further study of the adsorption of anti-BSA and glucose oxidase onto the surface of these BSA/PMMA particles for the development of high-performance biosensors.

Experimental Section

Materials. Bovine serum albumin was obtained from Amresco (purity ≥ 98%) and used without further purification. Methyl methacrylate (Shanghai Chemical Reagent) was first washed three times with a 5% sodium hydroxide solution to remove the inhibitor and then with deionized water until the pH of the water layer reached 7. Further, it was purified by vacuum distillation. $CuCl_2 \cdot 2H_2O$ (Shanghai Chemical Reagent) as well as chloroform and hydrochloric acid (Guangzhou Chemical Reagent) were used as received. Deionized water was used as the dispersion medium.

Synthesis of PMMA−BSA Core−Shell Particles. In a typical reaction, BSA (0.9278 g) was dissolved in 30 mL of deionized water at 25 °C in a water-jacketed flask equipped with a magnetic stirrer, a thermometer, a condenser, and a nitrogen inlet. After the solution mixture was stirred for 30 min, a designed amount of copper chloride aqueous solution was introduced. The stirred mixture was purged with nitrogen for 30 min prior to the addition of 3.7 g of MMA. The mixture was reacted for 3 h with constant stirring under nitrogen. The grafting PMMA−BSA copolymers as well as PMMA homopolymer inside the particles were isolated from the reaction mixture by a 72-h Soxhlet extraction with chloroform. The MMA conversion was determined gravimetrically. The extent of MMA conversion (MC), the grafting efficiency (GE), and the PMMA ratio on the copolymer (R_{PMMA}) are, respectively, calculated as follows: MC = $W_p/W_o \times 100\%$, GE = $W_g/W_p \times 100\%$, and $R_{PMMA} = [W_g/(W_g + W_b)] \times 100\%$, where W_o, W_p, W_g, and W_b are the weights of MMA monomers, total PMMA, PMMA grafted onto BSA, and BSA, respectively. Note that the presence of even such a trace amount of Cu^{2+} ions could be harmful for some bioapplications. It can be removed by repeated centrifugation because Cu^{2+} ions are highly soluble in water.

Copolymer Characterization. The infrared spectra were recorded on a FTIR-8300PCS spectrophotometer using a KBr disk. Thermogravimetric (TG) analysis was performed with Netzsch TG-409PC under flowing nitrogen (30 mL/min) at a heating rate of 10 °C/min.

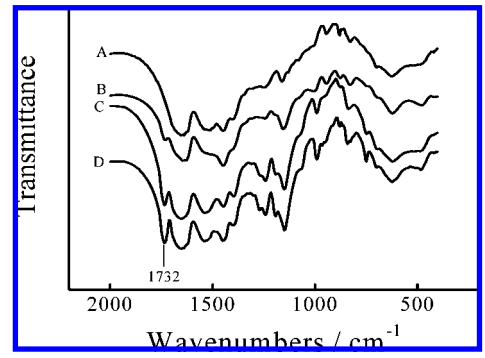

Figure 1. FTIR spectra of (A) BSA, (B) 23.2% grafted PMMA, (C) 43.6% grafted PMMA, and (D) 57.8% grafted PMMA.

The particle morphology was viewed with a JEOL JEM-1230 transmission electron microscope at an acceleration voltage of 80 kV. The transmission electron microscopy (TEM) sample was prepared by adding a drop of a dilute aqueous dispersion of PMMA−BSA particles on a carbon-coated copper grid. After 10 min, excess liquid was blotted away using a strip of filter paper, and further, a drop of 1% (w/w) phosphotungstic acid was added to the grid. After incubating at room temperature for 2 min, excess liquid was removed and the grid was dried at room temperature before the TEM analysis.

A commercial LLS spectrometer (ALV/DLS/SLS-5022F) equipped with a multi-τ digital time correlation (ALV5000) and a cylindrical 22 mW UNIPHASE He−Ne laser (λ_0 = 632.8 nm) as the light source was used. In dynamic LLS, the Laplace inversion of a measured intensity−intensity time correlation function $[G^{(2)}(t,q)]$ in the self-beating mode can result in a line-width distribution $G(\Gamma,q)$, where q is the scattering vector. For a pure diffusive relaxation, Γ is related to the translational diffusion coefficient D by $\Gamma/q^2 = D$ at $q \to 0$ and $C \to 0$, or to a hydrodynamic radius R_h by $R_h = k_BT/(6\pi\eta D)$ with k_B, T, and η being the Boltzmann constant, absolute temperature, and solvent viscosity, respectively. All the LLS measurements in this study were done at the scattering angle of 15° and the temperature of 25.0 ± 0.1 °C. For LLS, each solution was clarified by a 0.45-μM Millipore PTFE filter to remove dust.

Results and Discussion

Characterization of Grafting Copolymers. BSA-g-PMMA copolymers as well as PMMA homopolymer inside the core−shell particles were separated and isolated by Soxhlet extraction with chloroform for 72 h. The IR spectrum of the BSA-g-PMMA copolymer in Figure 1D (Samples B, C, and D were withdrawn at definite time intervals during the course of the reaction, where BSA 3 wt %, W_{MMA}/W_{BSA} = 4:1, and $[Cu^{2+}]$ = 5 μM) shows a strong absorption band at 1732 cm^{-1}, corresponding to the ester carbonyl group (>C=O) of PMMA, that is initially absent in pure BSA (Figure 1A). The absorption band at 1732 cm^{-1} increases as the copolymerization proceeds. It has been known that BSA can be completely hydrolyzed in 6 M HCl, but the loss of PMMA is very little under these conditions.[17,18] Therefore, the amount of PMMA grafted on BSA can be determined after treating BSA-g-PMMA with 6 M HCl for a week under reflux.

Figure 2 shows TG analysis curves of BSA, BSA-g-PMMA, and the grafted PMMA after the removal of BSA from BSA-g-PMMA by hydrolysis. BSA-g-PMMA shows an intermediate weight loss behavior in comparison with BSA or the grafted PMMA. A distinct two-step degradation process is observed for BSA-g-PMMA. As expected, the onset of the first weight loss at ~248 °C corresponds to the decomposition of BSA, while the second one at ~335 °C is related to the decomposition of the grafted PMMA. The extent of weight loss during the first stage approximately equals the BSA content in the resultant copolymer.

(24) Bontempo, D.; Heredia, K. L.; Fish, B. A.; Maynard, H. D. *J. Am. Chem. Soc.* **2004**, *126*, 15372–15373.
(25) Heredia, K. L.; Bontempo, D.; Ly, T.; Byers, J. T.; Halstenberg, S.; Maynard, H. D. *J. Am. Chem. Soc.* **2005**, *127*, 16955–16960.
(26) Liu, J.; Bulmus, V.; Herlambang, D. L.; Barner-Kowollik, C.; Stenzel, M. H.; Davis, T. P. *Angew. Chem., Int. Ed.* **2007**, *46*, 3099–3103.
(27) Boyer, C.; Bulmus, V.; Liu, J.; Davis, T. P.; Stenzel, M. H.; Barner-Kowollik, C. *J. Am. Chem. Soc.* **2007**, *129*, 7145–7154.

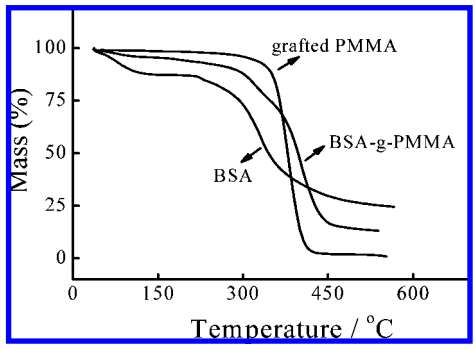

Figure 2. Thermogravimetric (TG) curves of BSA, BSA-g-PMMA copolymer, and grafted PMMA.

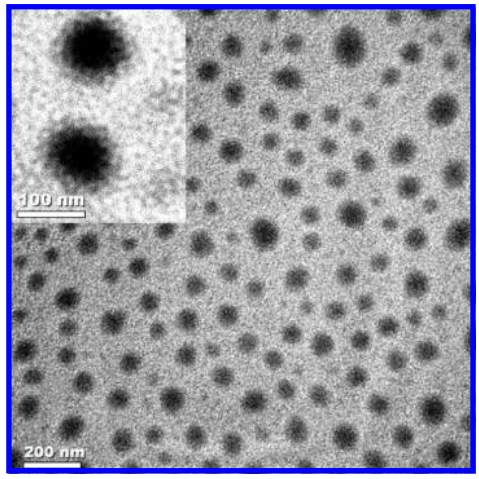

Figure 3. TEM images of PMMA−BSA particles stained with 1% phosphotungstic acid on carbon-coated grids.

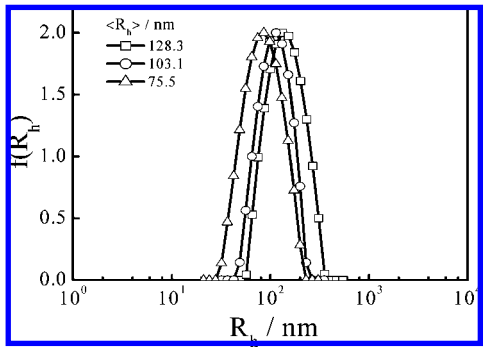

Figure 4. Typical hydrodynamic radius distribution $f(R_h)$ of PMMA−BSA particles in aqueous solution at 25 °C.

TEM images (Figure 3) reveal that such formed particles have some core−shell morphology, presumably with a water-insoluble PMMA core and a water-swollen BSA shell. The average radius of these core−shell particles estimated from TEM is in the range 40−60 nm, smaller than those obtained from dynamic LLS as shown in Figure 4, where $\langle R_h \rangle = 75.5$ nm. This is reasonable because the core−shell particles measured in TEM are dried and the BSA shell collapses after the evaporation of water, while the core−shell particles in dynamic LLS measurements have a swollen shell. Both TEM and dynamic LLS results reveal that such prepared core−shell particles are narrowly distributed. On the basis of the TEM micrograph, the estimated average radius of the PMMA core and the BSA shell thickness in the dried state are ∼25 nm and ∼30 nm, respectively. Note that the PMMA

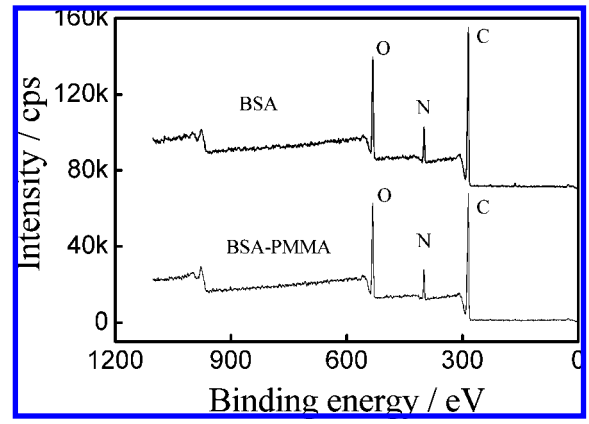

Figure 5. Respective XPS survey scans of pure BSA and BSA−PMMA particles.

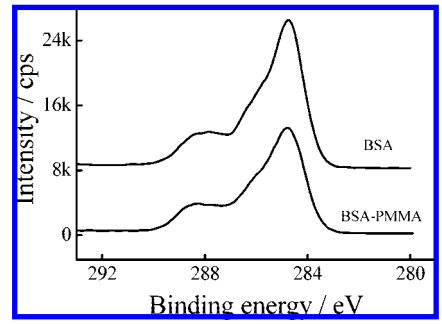

Figure 6. Respective high resolution C 1s spectra of pure BSA and BSA−PMMA particles.

Table 1. Effect of Reaction Temperature on the Graft Copolymerization of MMA from BSA, where $W_{BSA} = 3$ wt %, $W_{MMA}/W_{BSA} = 4{:}1$, and $[Cu^{2+}] = 5$ μM

temp/°C	MC (%)	GE (%)	R_{PMMA} (%)	$\langle R_h \rangle$/nm	$\mu_2/\langle \Gamma^2 \rangle$
70	7.1	85.7	19.6		
75	68.3	77.6	67.8	75.5	0.15
80	56.9	74.2	62.7	84.8	0.12
85	55.2	73.4	61.7	95.6	0.13

core also contains ∼20 wt % PMMA homopolymer chains formed and entrapped inside during the grafting copolymerization.

To prove that most of the BSA chains are indeed on the surface of resultant particles, namely, the particles have a core−shell structure, we performed the X-ray photoelectron spectra (XPS) by using a VGESCALAB MKII spectrometer with monochromatic Al Kα radiation as the excitation source. The binding energies obtained in the XPS analysis are standardized for specimen charging using C 1s as the reference at 284.6 eV. The surface composition was determined using the manufacturer's sensitivity factors. The results are respectively shown in Figures 5 and 6. The results of the XPS data analysis are listed in Table 4. Figures 5 and 6 reveal that the XPS survey scan of the BSA−PMMA particles is similar to that of pure BSA with their main peaks centered at 284.7, 399.6, and 531.6 eV, respectively, related to C 1s, N 1s, and O 1s. These results clearly show that, as expected, the surface of the BSA−PMMA particles is BSA. The high atomic percentage of N, as shown in Table 4, indicates that the BSA−PMMA particles must have a BSA shell thicker than the XPS sampling depth of ∼5 nm. In order to know the percentage of BSA molecule actually reacted, we prepared BSA−PMMA particles where $W_{BSA} = 3$ wt %, $W_{MMA}/W_{BSA} = 5{:}1$, and $[Cu^{2+}] = 5$ μM. The reaction mixture was diluted to an appropriate concentration and centrifugated three times to

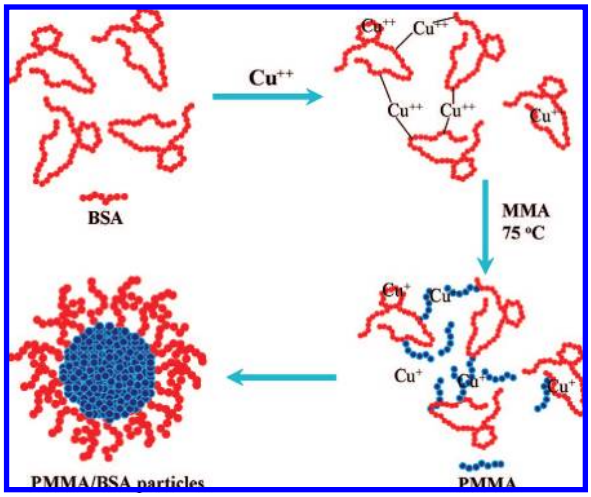

Figure 7. Schematic of the copper-mediated graft copolymerization of MMA from BSA.

Scheme 1. Kinetic Steps in the Cu^{2+}-Mediated Graft Copolymerization of MMA from the BSA Protein Chain at Higher Temperatures

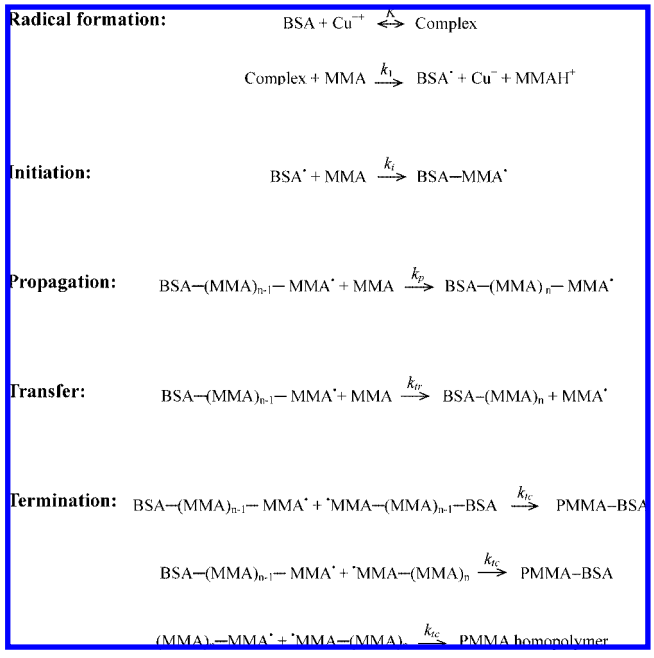

ensure removal of BSA−PMMA particles. The BSA concentration in the supernatant was determined according to the method reported by Bradford.[28] The percentage of BSA reacted in the reaction mixture was 91.7%.

Figure 7 shows a schematic of the Cu^{2+}-mediated graft copolymerization of MMA from water-soluble BSA chains. All the FT-IR, TG, and TEM results confirm that MMA monomers are indeed grafted on the BSA chain. We found that the addition of a trace amount of free radical inhibitor, *p*-dihydroxybenzene (0.2 mol % of MMA), in the reaction mixture can completely suppress the graft copolymerization, suggesting that the copolymerization in the presence of Cu^{2+} follows a free-radical mechanism, involving the complexation between BSA and MMA. A possible mechanism is described in Scheme 1.[29−37] After characterizing and confirming the structure of such obtained

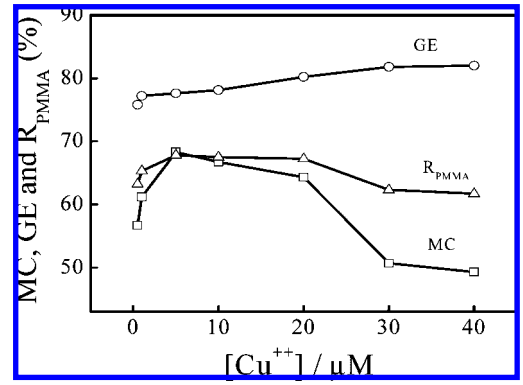

Figure 8. Effect of Cu^{2+} concentration on the MMA conversion (MC), grafting efficiency (GE), and grafting percentage (GP), where W_{BSA} = 3 wt % and W_{MMA}/W_{BSA} = 4:1 at 75 °C for 3 h.

core−shell particles, we focused on the optimal copolymerization conditions as follows.

Effect of Cu^{2+} Concentration. Figure 8 illustrates the effect of Cu^{2+} concentration on the MMA conversion (MC), the grafting efficiency (GE), and the PMMA ratio on the copolymer (R_{PMMA}) in the concentration range of $0.5 < [Cu^{2+}] < 40\ \mu M$, where other reaction conditions were kept identical. Both MC and R_{PMMA} initially increase as $[Cu^{2+}]$ increases up to 5 μM. Further increase of $[Cu^{2+}]$ in the range $\geq 10\ \mu M$ leads to their decrease. In the concentration range of $20 < [Cu^{2+}] < 30\ \mu M$, both MC and R_{PMMA} significantly drop. In contrast, the variation of $[Cu^{2+}]$ in the range 1−40 μM has little influence on the grafting efficiency. These results imply that the Cu^{2+}/BSA complexation induces the aggregation of BSA in an aqueous solution.[38,39] Dynamic LLS results reveal that the average hydrodynamic size of BSA is small when $[Cu^{2+}] < 10\ \mu M$ and presumably that BSA exists as individually soluble chains with more available reactive centers in the reaction mixture. It should favor the diffusion of MMA monomers to the active sites, resulting in a higher monomer conversion and a higher PMMA ratio on the copolymer chain. Further increase of $[Cu^{2+}]$ leads to larger Cu^{2+}/BSA aggregates. Some of the active sides on BSA are inevitably entrapped inside so that it is more difficult for MMA monomers to diffuse into these large aggregates and be initiated by those entrapped active sites. This explains why both MC and R_{PMMA} decrease. Note that there was no MMA polymerization in the absence of Cu^{2+}. Obviously, there exists a balance between the initiation of the graft copolymerization and the Cu^{2+}-induced BSA complexation. A proper trace amount of Cu^{2+} is required for the maximum effect on the graft copolymerization of MMA from BSA.

Effect of Cu^{2+} Concentration on Induction Time. Figure 9 shows the effect of $[Cu^{2+}]$ on the induction time of the graft copolymerization of MMA from BSA. The increase of $[Cu^{2+}]$

(28) Bradford, M. M. *Anal. Biochem.* **1976**, *72*, 248–254.
(29) Takata, T.; Takemoto, K. *Angew. Makromol. Chem.* **1971**, *19*, 1–14.
(30) Ouchi, T.; Yoshikawa, T.; Imoto, M. *J. Macromol. Sci., Chem.* **1978**, *12*, 1523–1547.
(31) Ouchi, T.; Kitazaki, S.; Kobayashi, A.; Imoto, M. *J. Macromol. Sci., Chem.* **1980**, *14*, 1045–1059.
(32) Ouchi, T.; Kobayashi, A.; Imoto, M. *J. Macromol. Sci., Chem.* **1982**, *17*, 771–790.
(33) Ouchi, T.; Watanabe, K.; Yoshikawa, T.; Morita, E.; Imoto, M. *Polym. J.* **1979**, *11*, 971–976.
(34) Ouchi, T.; Kuriyama, A.; Imoto, M. *Polym. J.* **1981**, *13*, 7–12.
(35) Imoto, M.; Ouchi, T. *JMS-REV. Macromol. Chem. Phys.* **1983**, *23*, 247–316.
(36) Gupta, K. C.; Sahoo, S.; Khandekar, K. *Biomacromolecules* **2002**, *3*, 1087–1094.
(37) Gupta, K. C.; Khandekar, K. *Biomacromolecules* **2003**, *4*, 758–765.
(38) Donato, L.; Garnier, C.; Doublier, J.-L.; Nicolai, T. *Biomacromolecules* **2005**, *6*, 2157–2163.
(39) Lin, W.; Zhou, Y.; Zhao, Y.; Zhu, Q.; Wu, C. *Macromolecules* **2002**, *35*, 7407–7413.

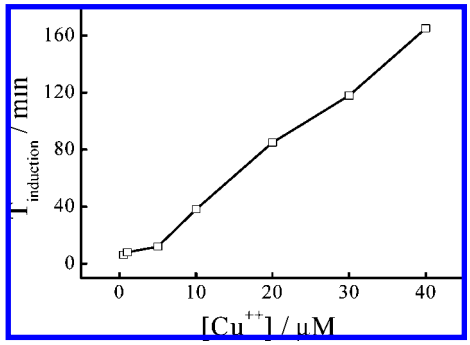

Figure 9. Effect of Cu^{2+} concentration on the induction time of the graft copolymerization of MMA from BSA where $W_{BSA} = 3$ wt %, $W_{MMA}/W_{BSA} = 4{:}1$, and $[Cu^{2+}] = 5$ μM at 75 °C for 5 h.

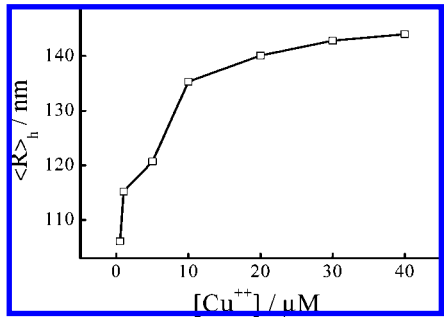

Figure 10. Effect of Cu^{2+} concentration on the average hydrodynamic radius $\langle R_h \rangle$ of the Cu^{2+}/BSA aggregates where $W_{BSA} = 3$ wt %.

Table 2. Effect of BSA Concentration on the Graft Copolymerization of MMA from BSA, Where $W_{MMA}/W_{BSA} = 4{:}1$ and $[Cu^{2+}] = 5$ μM at 75 °C

BSA (wt %)	MC (%)	GE (%)	R_{PMMA} (%)	$\langle R_h \rangle$/nm	$\mu_2/\langle\Gamma^2\rangle$
1	20.3	76.8	38.1	113.6	0.12
2	24.2	78.2	42.8	97.9	0.13
3	68.3	77.6	67.8	75.5	0.15
4	64.7	78.3	66.9	80.2	0.10
5	49.9	79.1	61.2	82.6	0.12
6	40.2	77.8	55.5		

leads to a significant increase of the induction time at ~5 μM. As previously described, Cu^{2+} can coordinate to nitrogen atoms on BSA in an aqueous solution to form intra- and interchain Cu^{2+}/BSA complexation.[40−44] As expected, the intrachain Cu^{2+}/BSA complexation leads to the contraction of individual BSA chains, while the interchain Cu^{2+}/BSA complexation results in the BSA aggregation. Such two processes compete with each other.[39] In the current study, the BSA concentration is fairly high (3 wt %) so that the interchain complexation becomes dominant, resulting in larger BSA aggregates.

Figure 10 shows that the average hydrodynamic radius ($\langle R_h \rangle$) of the Cu^{2+}/BSA aggregates increases with $[Cu^{2+}]$. Note that here there exist interchain and intrachain Cu^{2+}/BSA complexation. The interchain complexation leads to the aggregation of BSA, while the intrachain complexation results in the contraction of individual BSA chains. The induction time is closely related to the average size of the BSA aggregates. Two processes occur simultaneously. They have different effects on the final average particle size. The observed increase of $\langle R_h \rangle$ reveals that the interchain aggregation has a dominant effect. On the other hand, the intrachain contraction entrapped some active sites inside so that it must take a longer time for MMA monomers to diffuse and reach them. Our results reveal that using a lower Cu^{2+} concentration can reduce the induction time and favor the graft copolymerization of MMA from BSA, leading to a higher MC and R_{PMMA}, because individual BSA chains have a more open conformation.

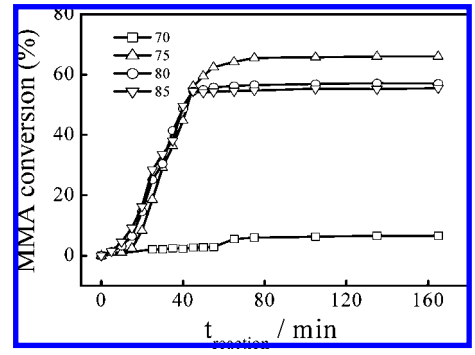

Figure 11. Reaction temperature dependence of the kinetics of the graft copolymerization of MMA from BSA where $W_{BSA} = 3$ wt %, $W_{MMA}/W_{BSA} = 4{:}1$, and $[Cu^{2+}] = 5$ μM.

Table 3. Effect of Weight Ratio of MMA to BSA on the Graft Copolymerization of MMA from BSA, Where $W_{BSA} = 3$ wt % and $[Cu^{2+}] = 5$ μM at 75 °C

W_{MMA}/W_{BSA}	MC (%)	GE (%)	R_{PMMA} (%)	$\langle R_h \rangle$/nm	$\mu_2/\langle\Gamma^2\rangle$
1:1	9.2	80.4	6.8		
2:1	33.3	79.1	34.5	63.7	0.16
3:1	58.6	77.3	57.6	72.6	0.16
4:1	68.3	77.6	67.8	75.5	0.15
5:1	72.7	73.4	72.7	82.6	0.12
6:1	73.2	72.8	76.1	103.1	0.10

Effect of Reaction Temperature. Table 1 shows the effect of the reaction temperature on the MMA conversion (MC), the grafting efficiency (GE), the PMMA ratio on the copolymer (R_{PMMA}), and the average size of resultant PMMA−BSA particles ($\langle R_h \rangle$) where other reaction conditions were kept identical. The shape increases of both MC and R_{PMMA} between 70 and 75 °C reveal that there exists an activation temperature close to 75 °C. Further increase of the reaction temperature leads to an unexpected decrease in the grafting efficiency, which is attributed to a higher chain transferring rate of free radicals to MMA monomers so that more PMMA homopolymer is produced at higher reaction temperatures. Table 1 also shows that the average particle size increases with the reaction temperature.

Figure 11 shows the reaction temperature dependence of the kinetics of grafting MMA from BSA. At 70 °C, only a small amount of MMA monomers are copolymerized on BSA. Further increase of the reaction temperature from 75 to 85 °C only has a slight effect on the initial reaction rate and the induction time but leads to a decrease in the final MMA conversion. In principle, the higher reaction temperature should lead to a faster reaction and a higher MMA conversion. However, BSA becomes more denaturalized and less soluble, resulting in larger Cu^{2+}/BSA aggregates. Therefore, MC decreases at higher reaction temperatures.

Effect of BSA Concentration. Table 2 shows that when [BSA] ≅ 3 wt %, both MC and R_{PMMA} reach their respective highest values. Further increase of the BSA concentration results in their slight decreases. This can be attributed to the increases of both the size of the Cu^{2+}/BSA aggregates and the viscosity of the

(40) Kolthoff, I. M.; Willeford, B. R. *J. Am. Chem. Soc.* **1958**, *80*, 5673–5678.
(41) Lal, H.; Narasinga Rao, M. S. *J. Am. Chem. Soc.* **1957**, *79*, 3050–3056.
(42) Lal, H. *J. Am. Chem. Soc.* **1959**, *81*, 844–848.
(43) Rakhit, G.; Antholine, W. E.; Froncisz, W.; Hyde, J. S.; Pilbrow, J. R.; Sinclair, G. R.; Sarkar, B. *J. Inorg. Biochem.* **1985**, *25*, 217–224.
(44) Laussac, J. P.; Sarkar, B. *Biochemistry* **1984**, *23*, 2832–2838.

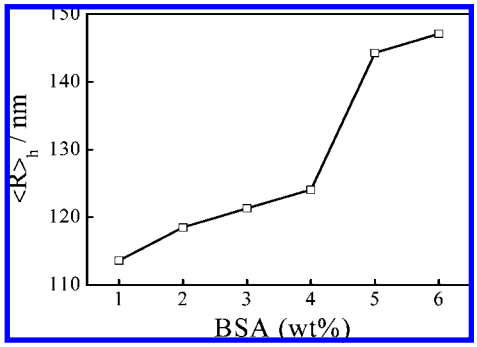

Figure 12. Effect of BSA concentration on the average hydrodynamic radius $\langle R_h \rangle$ of the Cu^{2+}/BSA aggregates where $[Cu^{2+}] = 5\ \mu M$.

Table 4. Atomic Compositions on Surfaces of Pure BSA and BSA−PMMA Particles

materials	C (%)	N (%)	O (%)
BSA	70.29	8.16	21.55
BSA−PMMA	68.49	7.45	24.08

reaction mixture (Figure 12); namely, the diffusion of MMA monomers to the reactive sites inside the Cu^{2+}/BSA complexes takes a longer time and becomes more difficult. Tobitani and Ross-Murphy[45] reported that the minimum gelation concentration of BSA is ~5% (w/w). In the current study, we observed that only heating a 6 wt % BSA solution mixture at 75 °C for 2 h can induce the sol−gel transition. Because the Cu^{2+} induced BSA intrachain contraction reduces the interchain association.

Effect of Weight Ratio of MMA to BSA. Table 3 shows the effects of the weight ratio of MMA to BSA on the MMA conversion (MC), the grafting efficiency (GE), the PMMA ratio on the copolymer (R_{PMMA}), and the average size of the resultant PMMA−BSA particles ($\langle R_h \rangle$). Both MC and R_{PMMA} increase with the MMA concentration but level off when W_{MMA}/W_{BSA} reaches 4−5. This is reasonable because when the MMA concentration increases, more MMA monomers are partitioned inside the Cu^{2+}/BSA complexes, so that more MMA can be grafted on BSA. On the other hand, the grafting efficiency slightly decreases as the MMA concentration increases.

The results in Tables 1−3 show that the PMMA−BSA core−shell particles formed under different reaction conditions are relatively narrowly distributed and the average particle size can be conveniently adjusted in the range 60−100 nm simply with a variation of the weight ratio of MMA to BSA. The optimal copolymerization temperature and the Cu^{2+} concentration are ~75 °C and 5 μM, respectively. The weight ratio (W_{MMA}/W_{BSA}) of MMA to BSA should be higher than 4. In general, the increase of W_{MMA}/W_{BSA} leads to higher MC, GE, and R_{PMMA}.

Conclusion

In the presence of a small amount of Cu^{2+}, MMA monomers can be grafted on a protein (BSA) chain via free radical copolymerization in water. The optimal reaction temperature is ~75 °C. The formation of PMMA homopolymer chains is reduced because free radicals are directly formed on the BSA chain. The grafting of hydrophobic PMMA on BSA makes the resultant copolymer amphiphilic. In the reaction mixture, such initially formed PMMA−BSA copolymer chains act as polymeric surfactants. The in situ association of these amphiphilic PMMA−BSA copolymer chains in water entraps and polymerizes more MMA monomers inside, resulting in the formation of narrowly distributed surfactant-free core−shell particles with a PMMA core and a BSA shell. The copolymerization after the initial stage is similar to an emulsion polymerization. The average particle size can be well controlled in the range 60−100 nm with a variation of the weight ratio of MMA to BSA. Such formed core−shell particle dispersions exhibit very good long-term stability and are potentially useful in bioapplications because of their inert and nontoxic PMMA core and biocompatible BSA shell.

Acknowledgment. The financial support of the Ministry of Science and Technology of China (2007CB936401), the National Natural Scientific Foundation of China (NNSFC; Projects 20574065 and 50333050), and the Hong Kong Special Administration Region (HKSAR; Earmarked Project CUHK4037/06P, 2160298) is gratefully acknowledged.

LA801132R

(45) Tobitani, A.; Ross-Murphy, S. B. *Macromolecules* **1997**, *30*, 4845–4854.